NEOPLASIA
www.neoplasia.com

Volume 14 Number 10 October 2012 pp. 943–951 943

Bone Marrow–derived Myofibroblasts Are the Providers of Pro-invasive Matrix Metalloproteinase 13 in Primary Tumor[1]

Julie Lecomte*, Anne Masset*, Silvia Blacher*, Ludovic Maertens*, André Gothot†, Marie Delgaudine†, Françoise Bruyère‡, Oriane Carnet*, Jenny Paupert*, Martin Illemann§,¶,#, Jean-Michel Foidart*, Ida K. Lund§,¶, Gunilla Høyer-Hansen§,¶ and Agnes Noel*

*Laboratory of Tumor and Development Biology, GIGA-Cancer, University of Liège, Liège, Belgium; †Laboratory of Haematology, GIGA Research Centre, University of Liège, Liège, Belgium; ‡Vesalius Research Center, Vlaams Instituut voor Biotechnologie, Katholieke Universiteit Leuven, Leuven, Belgium; §Finsen Laboratory, Copenhagen University Hospital, Copenhagen Biocenter, Copenhagen, Denmark; ¶Biotec Research and Innovation Center, University of Copenhagen, Copenhagen Biocenter, Copenhagen, Denmark; #Departments of Surgery, Medicine, and Oncology, McGill University Hospital Center, McGill University, Montreal, Canada

Abstract

Carcinoma-associated fibroblasts are key contributors of the tumor microenvironment that regulates carcinoma progression. They consist of a heterogeneous cell population with diverse origins, phenotypes, and functions. In the present report, we have explored the contribution of bone marrow (BM)–derived cells to generate different fibroblast subsets that putatively produce the matrix metalloproteinase 13 (MMP13) and affect cancer cell invasion. A murine model of skin carcinoma was applied to mice, irradiated, and engrafted with BM isolated from green fluorescent protein (GFP) transgenic mice. We provide evidence that one third of BM-derived GFP^+ cells infiltrating the tumor expressed the chondroitin sulfate proteoglycan NG2 (pericytic marker) or α-smooth muscle actin (α-SMA, myofibroblast marker), whereas almost 90% of $Thy1^+$ fibroblasts were originating from resident GFP-negative cells. MMP13-producing cells were exclusively $\alpha\text{-SMA}^+$ cells and derived from GFP^+ BM cells. To investigate their impact on tumor invasion, we isolated mesenchymal stem cells (MSCs) from the BM of wild-type and MMP13-deficient mice. Wild-type MSC promoted cancer cell invasion in a spheroid assay, whereas MSCs obtained from MMP13-deficient mice failed to. Our data support the concept of fibroblast subset specialization with BM-derived $\alpha\text{-SMA}^+$ cells being the main source of MMP13, a stromal mediator of cancer cell invasion.

Neoplasia (2012) 14, 943–951

Abbreviations: BM, bone marrow; CAF, carcinoma-associated fibroblast; MMP, matrix metalloproteinase; MSC, mesenchymal stem cell

Address all correspondence to: Agnes Noel, PhD, Laboratory of Tumor and Development Biology, University of Liège, Tour de Pathologie, CHU (B23), Sart-Tilman, B-4000 Liège, Belgium. E-mail: agnes.noel@ulg.ac.be

[1]This work was supported by grants from the European Union Framework Program Projects (FP7, "MICROENVIMET" No 201279), the Fonds National de la Recherche Scientifique (Belgium), the Federation belge contre le Cancer, the Fonds spéciaux de la Recherche (University of Liège), the Centre Anticancéreux près l'Université de Liège, the Fonds Léon Fredericq (University of Liège), the D.G.T.R.E. from the "Région Wallonne," and the Interuniversity Attraction Poles Program–Belgian Science Policy (Brussels, Belgium).
Received 6 July 2012; Revised 22 August 2012; Accepted 24 August 2012

DOI 10.1593/neo.121092

Introduction

Carcinoma growth and metastatic dissemination are dependent on the formation of a permissive tumor stroma composed of extracellular matrix (ECM) and heterogeneous population of activated stromal cells, including fibroblasts, endothelial cells, immune cells, and bone marrow (BM)–derived stem and progenitor cells [1,2]. These tumor-supporting stromal cells communicate with cancer cells through both paracrine and juxtacrine signals mediated by ECM component deposition, remodeling enzyme production, and growth factor or cytokine/chemokine secretion. The interactions occurring between tumor cells and host cells support blood vessel formation, promote the breakdown of physical matrix barrier, endow cancer cells with proliferative and invasive properties, and contribute to tumor cell attraction to distant organs [3].

Carcinoma-associated fibroblasts (CAFs) constitute the majority of stromal cells within the primary tumor in various types of carcinomas [4,5]. The term CAF remains poorly defined and covers a heterogeneous population of stromal cells displaying various phenotypes [5–7] that originate and develop mainly from the following three sources: 1) the recruitment of resident fibroblasts or stem cells from the surrounding tissue, 2) the epithelial-to-mesenchymal transition [8], or 3) the recruitment of BM-derived cells [9]. Studies on murine models have provided evidence that at least a portion of mesenchymal cells originates from BM-derived mesenchymal stem cells (MSCs) [10–12]. In *in vitro* experiments, human MSCs exposed to tumor-conditioned medium over a prolonged period of time have been shown to assume a CAF-like myofibroblastic phenotype, suggesting that MSCs are a source of CAFs and can be used in the modeling of tumor-stroma interactions [13]. It is, however, not known whether these fibroblast subpopulations are equally important to support tumor progression or whether certain subpopulations contribute to specific steps of tumor growth, invasion, and metastases. Notably, the elegant study of Karnoub et al. has highlighted the contribution of MSCs to metastatic dissemination of cancer cells [14]. How MSCs endow malignant cells with a metastatic potential is still not fully understood.

CAFs acquire a reactive phenotype similar to fibroblasts observed during wound healing with the difference that they remain constantly activated [15]. Activated fibroblasts are commonly identified by their expression of α-smooth muscle actin (α-SMA), leading to the term "myofibroblasts." They synthesize a large amount of ECM components [4] and contribute to ECM turnover by secreting a number of ECM-degrading proteases such as the matrix metalloproteinases (MMPs) [16]. Among MMPs, the collagenase subfamily contributes to matrix remodeling by their ability to degrade fibrillar collagens [16]. This subfamily includes the fibroblast interstitial collagenase (MMP1), neutrophil collagenase or collagenase 2 (MMP8), and collagenase 3 (MMP13). In addition, MMP14 (MT1-MMP) and gelatinases A and B (MMP2 and MMP9) display collagenolytic activities [17,18]. These enzymes might exert opposite functions during cancer progression, as some of them (e.g., MMP8) have a protective role in cancer [19], whereas others (e.g., MMP1 and MMP13) promote tumor progression [20].

The human form of MMP13 was initially identified in breast cancer tissue [21] and has been detected in a large set of invasive neoplastic tumors [22–26]. MMP13 expression is detected in tumor cells at the invading front [22] and in stromal fibroblasts adjacent to tumor cells [26]. The mouse counterpart of MMP13 is also strongly expressed in the stroma of breast cancer xenografted tumor [27] and mammary carcinomas [28]. In a xenograft mouse model of skin squamous cell carcinoma, MMP13 was shown to enhance tumor growth and to promote angiogenesis through the release of vascular endothelial growth factor from the ECM, thus allowing the invasive growth of skin squamous carcinoma cells [29]. The implication of BM-produced MMP13 in angiogenesis was also pointed out during choroidal neovascularization in a mouse model of age-related macular degeneration [30].

In the present study, we investigated the involvement of BM-derived MSCs in the establishment of skin carcinoma-associated fibrovascular network. By studying different mesenchymal markers, as the fibroblast marker Thy1, the myofibroblast marker α-SMA, and the perivascular marker NG2, we provide evidence that BM-derived MSCs contribute to fibroblastic populations associated with the connective travea as well as to pericytic subpopulation surrounding blood vessels. Notably, we provide evidence that MMP13 is produced by a specialized subset of tumor-infiltrating myofibroblasts expressing α-SMA and derived from BM-MSCs.

Materials and Methods

Transgenic Mice

Transgenic mice heterozygous for the enhanced green fluorescent protein (GFP) under the control of β-actin promoter C57BL/6-Tg (ACTbEGFP)10sb were obtained from Jackson Laboratories (Bar Harbor, ME). Homozygous Mmp13-deficient mice ($Mmp13^{-/-}$) and the corresponding wild-type mice (WT) were generated in C57BL/6 background as previously described [30,31]. Mouse experimental procedures were performed in accordance with the guidelines of the University of Liège regarding the care and use of laboratory animals.

MSC Isolation and Characterization

MSCs were isolated from the BM and compact bones, isolated from 8- to 10-week-old mice, by crushing the mouse femurs and tibias with mortar and pestle in phosphate-buffered saline (PBS) containing 2% FBS and 1 mM EDTA. Cell suspension was collected and the remaining bone fragments were incubated in 0.25% collagenase 1a (Sigma-Aldrich, St Louis, MO) in PBS containing 20% FBS at 37°C. After 45 minutes of incubation, the cells were harvested, pooled with the initial cell suspension, and cultured in mouse MesenCult medium (STEMCELL Technologies, Grenoble, France) under hypoxic conditions (5% O_2). The cells were checked for MSC marker expression ($CD106^+$, $Sca1^+$, $CD34^-$, $CD45^-$, and $CD11b^-$) by flow cytometry and for their capacity to differentiate into adipocytes, osteocytes, and chondrocytes, as previously described [30]. We consider a culture as being MSC when at least 90% of cells express CD106 and Sca1 and do not express CD34, CD45, and CD11b. Moreover, the cells must differentiate into adipocyte, osteocyte, or chondrocyte when cultured in appropriate medium. The colony forming unit–fibroblast (CFU-F) assay was used as a functional method to quantify MSCs [32]. MSCs were used between passages 5 and 10.

BM Transplantation

BM cells were isolated from the tibia and femur of 8- to 10-week-old donor GFP mice, by slowly flushing Dulbecco's modified Eagle's medium (DMEM) culture medium (Gibco BRL, Paisley, United Kingdom) inside the diaphyseal channel and then intravenously injected into 8- to 10-week-old recipient C57Bl/6 mice (10^7 BM cells per animal), which before had been sublethally irradiated with a single dose of

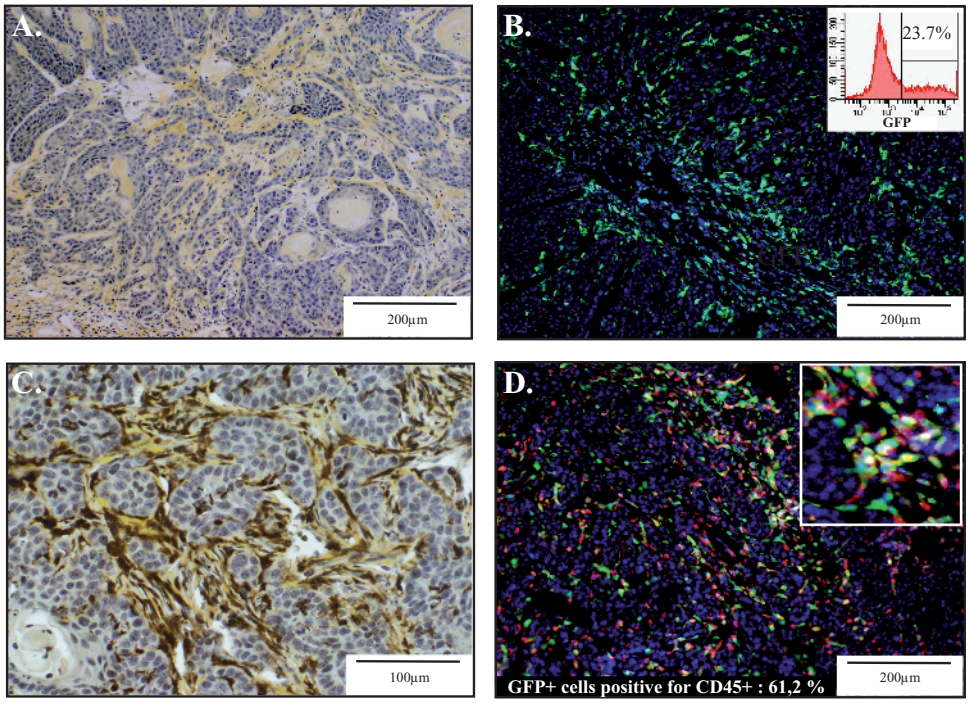

Figure 1. BM-derived cells recruited in the stroma of skin tumors. PDVA malignant keratinocytes were transplanted into mice engrafted with BM from GFP transgenic mice. (A) Intense desmoplastic reaction evidenced within the skin tumor by collagen staining using saffron coloration (yellow). (B) GFP^+ BM–derived cells recruited in the tumor. Flow cytometry analysis of cells isolated from the tumor through enzymatic dissociation revealing that 23.7% of cells were GFP^+ (insert). (C) Combined GFP immunoperoxidase staining of GFP^+ cells (brown) and collagen deposition through saffron coloration (yellow). (D) Detection of GFP positivity (green) and immunostaining for $CD45^+$ inflammatory cells (red). A higher magnification is shown (insert). The percentage of $CD45^+$ cells expressing GFP was assessed by a computerized method of quantification.

9 Gy. The success of BM transplantation was assessed by flow cytometry on blood and BM samples were collected at the end of the experiment to determine the percentage of GFP^+ cells. For all assays, similar percentage of BM reconstitution (around 70%) was observed. Engraftment of MSCs was assessed through MSC isolation and characterization, as described above, 5 weeks after the graft. *In vitro* CFU-F assay revealed that one third of MSCs were GFP^+ cells (data not shown).

Subcutaneous Tumor Injection Model

Malignant murine keratinocytes (PDVA cells) were generated by *in vitro* treatment of B10LP mouse keratinocytes with a carcinogen (7,12-dimethylbenz(a)antracene) [33]. Five weeks after BM transplantation (described above), the PDVA cancer cells (10^6 cells/injection) were subcutaneously injected in both flanks of the mouse (n = 33). On day 45, the tumors were resected, fixed in 4% paraformaldehyde, incubated in 30% sucrose solution, and frozen in cold 2-methylbutane for cryostat sectioning (6 µm in thickness) or fixed in 4% formamide for paraffin embedding.

Immunohistochemistry

For immunofluorescence, cryostat sections were fixed in 4% paraformaldehyde before incubation with primary antibodies. Antibodies raised against NG2 chondroitin sulfate proteoglycan (rabbit anti-rat antibody; Chemicon, Temecula, CA), α-SMA/Cy3 (Sigma-Aldrich), and Thy1 (rat anti-mouse antibody; BD Pharmingen, Franklin Lakes, NJ) were incubated for 1 hour at room temperature. After washings, the secondary swine anti-rabbit antibody conjugated to Texas Red was applied for NG2 labeling (Dako, Glostrup, Denmark) for 30 minutes. For Thy1 labeling, slides were incubated with biotin-coupled rabbit anti-rat antibody (Dako) for 30 minutes, washed, and incubated with streptavidin/Alexa Fluor 555 (Invitrogen, Carlsbad, CA) for 30 minutes.

For combination of GFP immunoperoxidase with hematoxylin and saffron staining, cryostat sections were first incubated with anti-GFP antibodies (rabbit polyclonal antibody, 1/200; Abcam, Cambridge, United Kingdom) for 1 hour, followed by incubation with swine anti-rabbit HRP (Dako). After Mayer's hematoxylin (Biogenex, Fremont, CA) coloration, the slides were dehydrated in ethanol and stained for 30 minutes with alcoholic safranin O (0.6% safranin in 20% ethyl alcohol; Sigma-Aldrich) before mounting.

For quantitative measurements of BM-derived cell infiltration in the tumor, automatic computer-assisted image analysis was done on images obtained after double immunostainings (five sections per tumor, number of tumors = 8). Original stained images were registered in red-green-blue. Red and green image components were processed independently and transformed in gray level images. Each component was binarized using an automatic threshold to extract cells from the background. The areas occupied by each cell subtype as well as the intersection areas were calculated. Results are presented as the common area occupied by BM-derived GFP^+ cells (in green) and immunostained cells (cells positive for α-SMA, NG2, or Thy1; in red) reported to the immunostained area. The relevance of the image analysis applied here was assessed by a multiscale validation (at 10- and 20-fold magnification). Results presented are those obtained at 10-fold magnification.

In Situ *Hybridization*

Antisense and sense MMP13 riboprobes were generated from plasmid pCLM11-810 [34] as previously described [35]. The exposure time in nuclear emulsion (ILFORD Imaging UK Limited, Mobberley, United Kingdom) was 7 days. Combined immunohistochemistry and *in situ* hybridization were performed according to Illemann et al. [36]. Hence, before the *in situ* hybridization, the primary antibody [α-SMA/fluorescein isothiocyanate (FITC; Sigma-Aldrich) or GFP (Abcam)] diluted in PBS containing 1% RNAse inhibitor was incubated for 2 hours at room temperature (Roche, Basel, Switzerland). Incubation with radiolabeled probe (sense or antisense) was then performed as specified above. Finally, the sections were counterstained with Mayer's hematoxylin, dehydrated with ethanol, and mounted.

To determine the distribution of MMP13 mRNAs in relation with α-SMA$^+$ or GFP$^+$ cells detected by immunohistochemistry, we applied a computer-assisted quantification method described previously [37]. The skeleton of immunopositive stromal compartment was first delineated. The density of black spots (MMP13 mRNAs) was then calculated in successive rings obtained by the dilatation 1, 2, …, *n* times of these skeletons. The density of labeling cells is represented in a function of the distance to stromal compartment skeleton.

Tumor Cell Dissociation and Flow Cytometry Analysis

Whole tumor samples were cut into small pieces and treated during 30 minutes at 37°C with type 1a collagenase from *Clostridium histolyticum* (400 U/ml; Sigma-Aldrich) and DNAse (1 mg/ml; Roche) to dissociate the tumor into single-cell suspension. The cell suspension was filtered (40-μm cell strainer; BD Falcon, San Jose, CA) and analyzed by flow cytometry for GFP expression using a FACSCanto II cell sorter (BD Biosciences, San Jose, CA).

Confrontation of Tumor Cells and MSC in Culture

Multicellular spheroids were generated by seeding 2000 PDVA cells alone or with 2000 MSCs in each well of nonadherent round-bottomed 96-well plates, in DMEM (Gibco BRL) containing 2% FBS and 0.24% high-viscosity methylcellulose (Sigma-Aldrich). After 24 hours of culture, spheroids were collected (maximum of eight per well), embedded in collagen gels in 48-well plates, and maintained in 2% FBS DMEM at 37°C for 48 hours. In some assays, a broad-spectrum hydroxamic acid–based synthetic MMP inhibitor BB-94 [38] was added at a final concentration of 5 μM in the collagen gel and in the culture medium. Cells were examined under a Zeiss Axiovert 25 microscope equipped with an Axiocam Zeiss camera and KS 400 Kontron image analysis software (Carl Zeiss Microscopy, Zaventem, Belgium). Images were processed using ImageJ program to become binary images in which the value of 1 was attributed for cells and the value of 0 for the background. Results are presented as the total migrating cell area reported to spheroid area. In co-culture assays, MSCs were cultured on six-well plates (250,000 cells/well) in the absence or presence of a 0.4-μm pore size insert (Greiner Bio One, Alphen aan den Rijn, The Netherlands) containing PDVA cells (50,000 cells/insert). These inserts allow the passage of soluble factors but not cells to migrate. After 3 days of culture, MSCs were harvested for protein or RNA extractions.

RNA Extraction and Reverse Transcription–Polymerase Chain Reaction

Total RNA from MSC and PDVA cells were extracted using the High Pure RNA Isolation Kit (Roche Diagnostics, Mannheim, Germany) according to the manufacturer's protocol. Reverse transcription–polymerase chain reaction (RT-PCR) was performed using an amplification kit (GeneAmp Thermostable rTth Reverse Transcriptase RNA

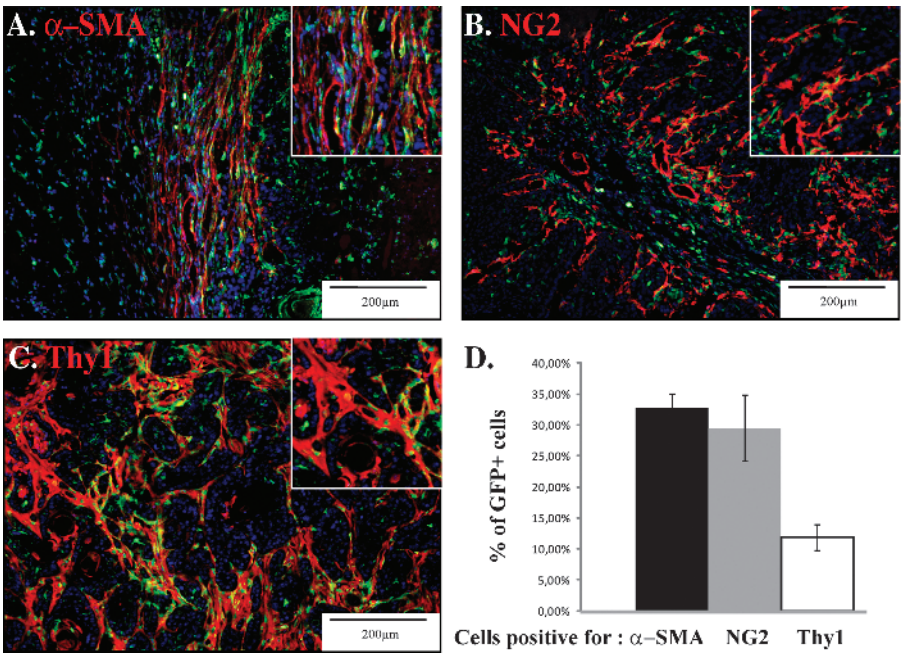

Figure 2. Characterization of BM-derived fibroblastic cell subsets in the tumor. PDVA malignant keratinocytes were subcutaneously transplanted into both flanks of mice, which have been engrafted with BM derived from GFP transgenic mice. Representative images of cryosections of squamous cell carcinoma tumor tissue infiltrated with GFP$^+$ BM–derived cells (green) and immunostained for the presence of (A) α-SMA, (B) NG2, and (C) Thy1 (red). A higher magnification is shown (insert). (D) Computerized quantification of the co-localization of GFP signal with α-SMA, NG2, and Thy1 immune signals.

PCR Kit; Roche, Branchburg, Germany). Specific pairs of primers (Eurogentec, Seraing, Belgium) for mouse MMP13 were designed as follows: forward (exon 6), 5′-ATGATCTTTAAAGACAGATTCT-TCTGC-3′; reverse (exon 7), 5′-TGGGATAACCTTCCAGA-ATGTCATAA-3′. Amplification of 32 cycles was run for 15 seconds at 94°C, 20 seconds at 68°C, and 30 seconds at 72°C followed by a final 2-minute extension step at 72°C. RT-PCR products were resolved in 10% acrylamide gels and analyzed with a fluorescence imager (LAS-4000; Fujifilm, Tokyo, Japan) after staining with Gel Star (Cambrex, East Rutherford, NJ). Gene expression levels were measured as a ratio between expression values and internal 28S.

Protein Extraction and Western Blot

After cell incubation in ice-cold lysis buffer (1% Triton X-100, 150 mM NaCl, 1% IGEPAL-CA 630, 1% sodium deoxycholate, 0.1% sodium dodecyl sulfate (SDS), complete) for 30 minutes, cell lysates were clarified by centrifugation at 12,000 rpm at 4°C for 30 minutes and stored frozen at −20°C. Protein concentration was determined by using DC Protein Assay Kit (Bio-Rad Laboratories, Hercules, CA). Protein samples were electrophoresed on gradient sodium dodecyl sulfate–polyacrylamide gel and subsequently transferred to polyvinylidene fluoride membranes. Membranes were treated with blocking buffer [PBS 0.1% Tween-20 (Merck, Whitehouse Station, NJ), 1% casein (Sigma-Aldrich)] for 1 hour at room temperature and followed by incubation with a sheep anti-mouse MMP13 (sheep polyclonal to MMP13 diluted 1/700; Abcam) overnight at 4°C. After extensive washings, membranes were incubated for 1 hour with secondary HRP antibodies (rabbit anti-sheep/HRP diluted 1/2000; Dako). Bands were detected by chemiluminescence using an Enhanced Chemiluminescence Kit (Perkin Elmer Life Sciences, Boston, MA) according to the manufacturer's instructions. Subsequent detection of actin (rabbit anti-actin; Sigma-Aldrich) was performed on the same filters as control.

Statistical Analysis

Data were analyzed with GraphPad Prism 4.0 (San Diego, CA). The Mann-Whitney test was used to determine whether differences between experimental groups could be considered as significant ($P < .05$).

Results

BM-derived Cells Recruited in the Tumor Stroma Fuel the Generation of CAFs with Different Phenotypes

To determine how BM-derived cells contribute to stromal support in tumor growth of squamous cell carcinoma of the skin, we used a murine malignant keratinocyte cell line (PDVA) transplantation mouse model in C57Bl/6 mice irradiated and grafted with unfractionated BM derived from GFP transgenic mice. Five weeks after transplantation, BM engraftment was confirmed through flow cytometry analysis. Moreover, among BM-engrafted cells, the MSC population also replenished the BM, as assessed by MSC isolation from BM of chimeric mice. The CFU-F assay revealed the presence of one-third GFP^+ MSCs within the BM of recipient mice (data not shown), thus donor-derived, consistent with previously published studies [39,40]. At this time point, PDVA cells were subcutaneously injected into mice flanks. The histologic examination of tumors harvested at day 45 revealed the presence of spindle-shaped fibroblastic cells, organized in bundles in collagen-containing stromal septa infiltrating the

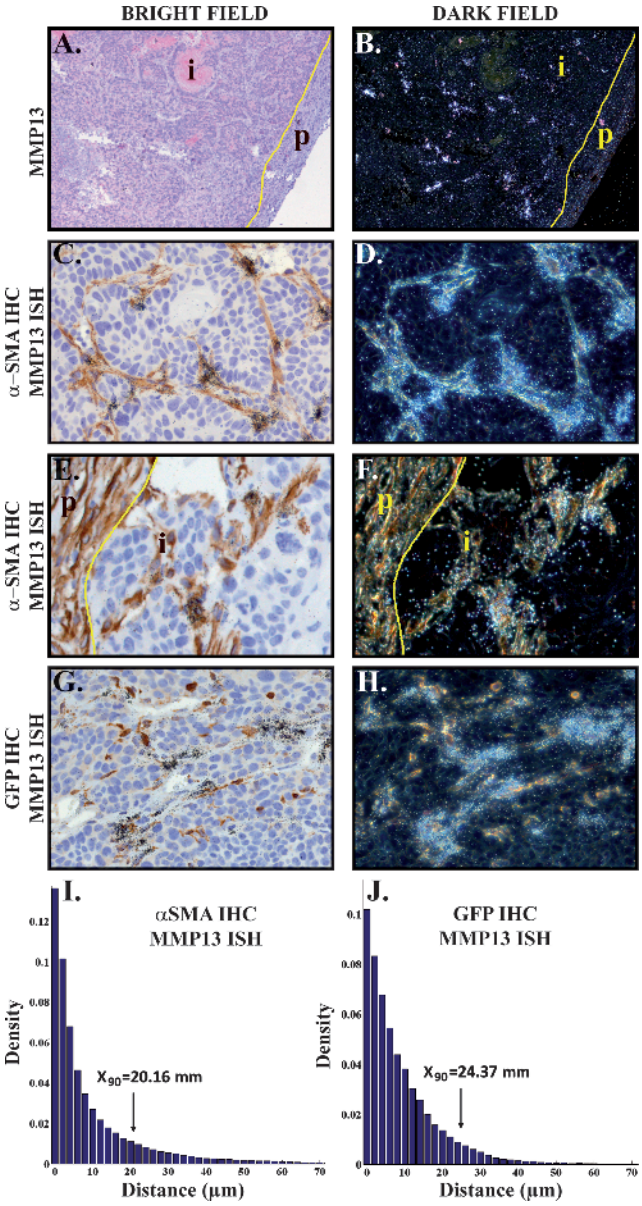

Figure 3. Expression of MMP13 by BM-derived myofibroblasts. (A, B) MMP13 *in situ* hybridization demonstrated strong expression of MMP13 mRNA by stromal cells invading the tumor, whereas stromal cells bordering the tumor presented lower signal. (C, D) A combination of α-SMA immunostaining and MMP13 *in situ* hybridization revealed that MMP13 mRNA is expressed by myofibroblasts. (E, F) α-SMA–positive myofibroblasts bordering the tumor express only low amounts of MMP13 mRNA, whereas myofibroblasts within the tumor mass do express high amounts of MMP13 mRNA. (G, H) The expression of MMP13 by GFP^+ BM–derived cells was illustrated by a combination of MMP13 *in situ* hybridization and GFP immunostaining. Representative images of *in situ* hybridization without and combined with immunoperoxidase stainings are presented in bright field (A, C, E, and G) and in dark field (B, D, F, and H); i, intratumoral; p, peritumoral. The graphs correspond to the density of MMP13 mRNA labeling as a function of the distance to brown staining of (I) α-SMA or (J) GFP. X_{90} (percentile) means that 90% of values are below this distance.

tumor and evidenced by saffron staining (Figure 1*A*). Morphologic features of these tumors resembled the desmoplastic reaction usually seen in human invasive skin carcinomas.

GFP-positive cells were observed in the entire tumor (Figure 1*B*) and mainly associated with the connective tissue bundles, as assessed by combined immunostaining for GFP and saffron staining (Figure 1*C*). Flow cytometry analysis of the cell suspension obtained from enzymatic tumor dissociation revealed that 23.7% of cells infiltrating the tumor were GFP^+-derived cells (insert in Figure 1*B*). A large proportion of the GFP^+ cells (61%) were inflammatory $CD45^+$ cells (Figure 1*D*). Furthermore, the following three different mesenchymal markers were used to determine the proportion of the different stromal subpopulations that originate from the BM: α-SMA for myofibroblastic cells (Figure 2*A*), NG2 for pericytes (Figure 2*B*), and Thy1 for fibroblastic-like cells (Figure 2*C*). A computer-assisted quantification method revealed that $\alpha\text{-SMA}^+$ cell population contained at least 30% of GFP^+ cells that were BM-derived cells. A similar fraction of the GFP^+ BM–derived cells were positive for NG2, whereas only a small proportion (less than 10%) was Thy1 immunoreactive (Figure 2*D*). These results demonstrate a recruitment of CAFs from the BM and that each fibroblastic subset consisted of a mixed population of cells obtained from BM-derived cells and resident fibroblasts with $Thy1^+$ cells mainly originating from local cells. Notably, few if any double-positive (GFP/α-SMA, GFP/Thy1, or GFP/NG2) cells were found in the normal skin (data not shown).

MMP13 Is Expressed by α-SMA–Positive Cells Derived from the BM

We next analyzed the expression of MMP13 in BM-derived cells through *in situ* hybridization using ^{35}S-labeled MMP13 riboprobes. MMP13 *in situ* hybridization was combined to α-SMA or GFP immunostainings. For all samples, a corresponding sense probe was used as negative control and showed only background signal (data not shown). MMP13 mRNA was detected in all samples (n = 19) and was localized in the stroma at invasive foci of the tumor (Figure 3, *A*–*D*). A faint MMP13 mRNA staining was detected in the peritumoral area, whereas a strong staining was found in intratumoral stromal bundles (Figure 3, *A* and *B*). When α-SMA immunostaining was combined to MMP13 *in situ* hybridization, MMP13 mRNA expression was exclusively detected in myofibroblasts infiltrating the tumor (Figure 3, *C*–*F*). GFP immunostaining combined to MMP13 *in situ* hybridization revealed that MMP13 mRNA was expressed by BM-derived cells (Figure 3, *G* and *H*). A computer-assisted quantification method was used to determine the association between α-SMA– or GFP-positive cells and the expression of MMP13 mRNA. The distribution of MMP13 mRNAs in and around α-SMA– or GFP-positive stromal compartment showed that 90% of MMP13 mRNAs are at a distance maximum of 24.37 μm from GFP-positive cells (X_{90} = 24.37 μm) and 20.16 μm from α-SMA–positive cells (X_{90} = 20.16 μm). These results therefore demonstrate that MMP13 is produced by BM-derived $\alpha\text{-SMA}^+$ myofibroblasts (Figure 3, *I* and *J*).

MSC-derived MMP13 Promotes Cancer Cell Invasion In Vitro

With the aim to determine whether MSC-derived MMP13 could influence cancer cell invasion, MSCs were isolated from mouse BM and used *in vitro*. The expression of MMP13 was evaluated both at the mRNA and protein levels in cultures of MSCs alone or with PDVA cancer cells separated by a semipermeable membrane, allowing the passage of secreted molecules. Both MMP13 mRNA and protein levels of MSCs were significantly increased, when PDVA cells were present (Figure 4). Western blot analyses revealed that both pro-form of 60 kDa and an active species of 48 kDa were detected upon MSC confrontation to soluble factors produced by cancer PDVA cells (Figure 4*B*). No mRNA for murine collagenase 1A, the mouse counterparts of human MMP1, was detected in MSC cultures, neither in the absence nor in the presence of PDVA cells. MSCs expressed low levels of MMP2 and MMP14 mRNAs that were not modulated upon confrontation to cancer cells (Figure 4*A*).

The putative pro-invasive effects of MSC-derived MMP13 on invasive capacity of PDVA cancer cell were examined using an *in vitro*

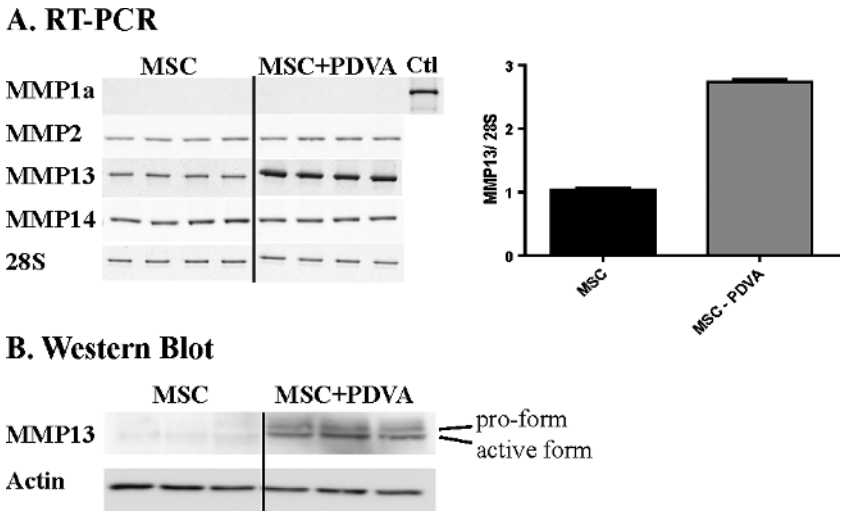

Figure 4. Malignant keratinocytes stimulate MMP13 expression of MSC. (A) MSCs were cultured alone (MSC) or in the presence of an insert containing PDVA cancer cells (MSC + PDVA). (A) RT-PCR analyses of different MMPs. Quantification of MMP13 mRNA levels modulated upon MSC to cancer cell confrontation is expressed as a ratio between MMP13 mRNA and 28 rRNA (graph on the right panel). A positive control (corresponding to murine placenta) is shown for MMP1a mRNA analysis (Ctl). (B) Western blot analysis of MMP13 pro-form and active form expression by MSCs cultured with PDVA cells. Actin was used as a loading control.

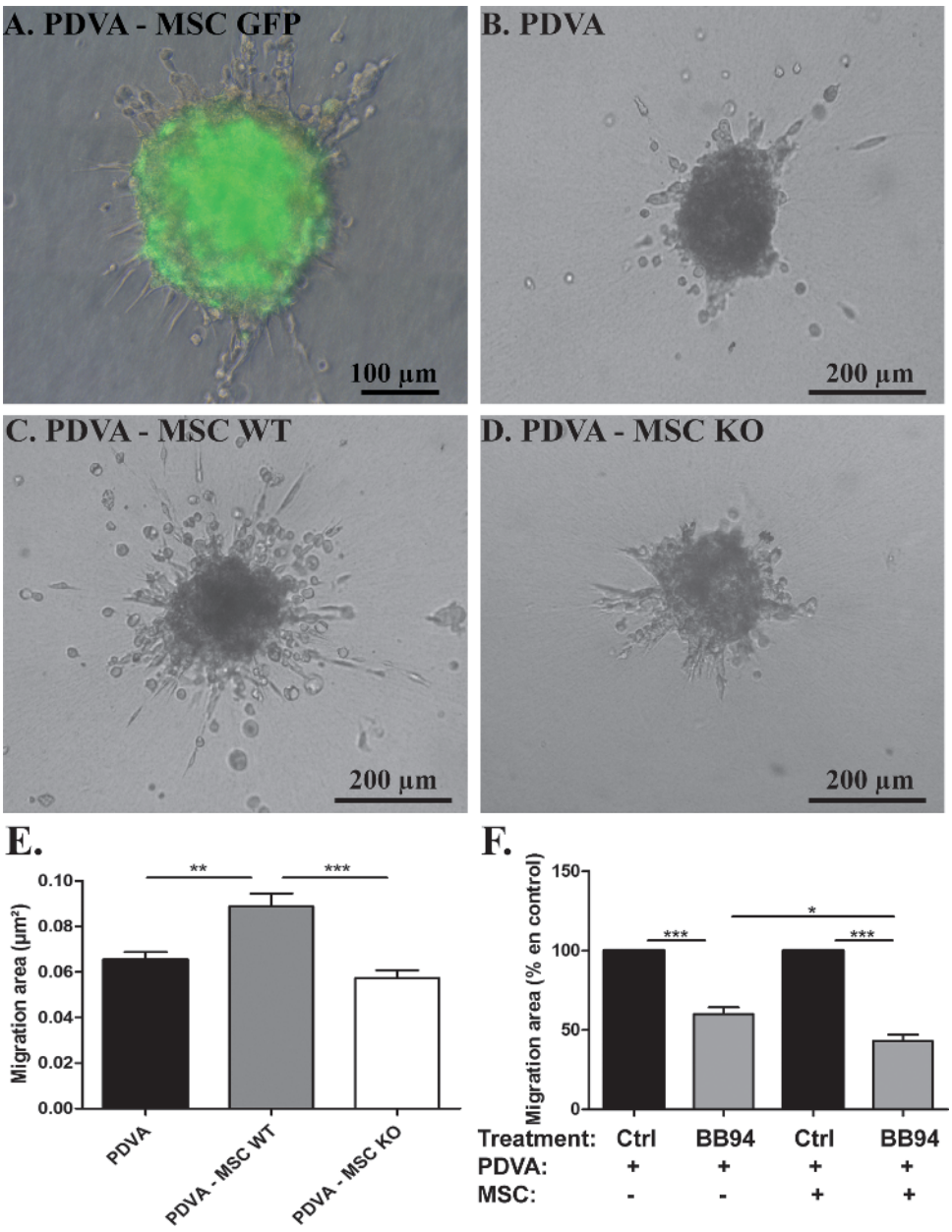

Figure 5. MSC-derived MMP13 promotes cancer cell migration in a three-dimensional spheroid model. PDVA cells alone (PDVA) or mixed with MSC (PDVA + MSC) were embedded as spheroids in a type 1 collagen matrix for 48 hours. MSCs were derived from (A) GFP mice, (C) wild-type mice (MSC WT), or (D) MMP13-deficient mice (MSC KO). (A) Combination of fluorescent and phase contrast images showed that GFP signal is detected in the spheroids composed of PDVA and GFP$^+$ MSC but not in cells spreading out of the spheroid. Optical microscopic observation of spheroids composed of PDVA alone (B) or confronted to MSC expressing (C) or not MMP13 (D). (E) Quantification of tumor cell migration area of PDVA cells cultured alone or mixed with MSC WT or MSC KO. (F) Quantification of PDVA cell migration area cultured alone or mixed with MSC, in the presence of BB94 or control.

spheroid migration assay. MSCs were isolated from GFP$^+$ mice, wild-type mice, or MMP13-deficient mice. The production of MMP13 in wild-type mice but not in MMP13-deficient mice was assessed at both mRNA and protein levels (data not shown). When PDVA cells were confronted with GFP$^+$ MSCs in spheroids embedded in a collagen gel, cancer cells sprouted into the matrix, whereas MSCs remained in the spheroid (Figure 5*A*). Malignant cell invasion was significantly enhanced in the presence of MSCs compared to PDVA cells cultured alone ($P = .0032$; Figure 5, *B* and *C*). Notably, the presence of MSCs harvested from MMP13-deficient mice did not stimulate PDVA cell migration in the spheroid assay, demonstrating the contribution of MSC-derived MMP13 in PDVA cell migration (Figure 5, *D* and *E*). We also evaluated the impact of a broad-spectrum MMP inhibitor (Batimastat or BB94). While BB94 reduced by 40% PDVA cell migration in monoculture, a higher inhibition (57%, $P < .05$) was observed in the presence of MSC (Figure 5*F*).

Discussion

Carcinoma cells are not self-sustaining entities, but their proliferative and invasive capacities are influenced by stromal cells derived from several sources. Although CAFs are now recognized as a heterogeneous

cell population, the correlation between their origin, phenotype, and function remains unclear. Here, through the engraftment of GFP$^+$ BM into mice, we show that 1) BM-derived cells infiltrate murine skin carcinomas and generate inflammatory cells and CAFs positive for α-SMA, NG2, or Thy1; 2) each fibroblastic population derives from cells of two different origins, i.e., BM-derived progenitors and tissue-resident cells; 3) at least one third of α-SMA– or NG2-positive cells are BM-derived cells, whereas Thy1$^+$ fibroblasts are primarily derived from resident cells; 4) MMP13 is produced by BM-derived α-SMA myofibroblasts; 5) MSC-derived MMP13 promotes cancer cell invasion.

In accordance with previous reports [41], by providing evidence in a murine skin carcinoma that the tumor stroma is composed of a combination of host and BM-derived fibroblastic cells, our study supports the concept that cancer is a systemic disease rather than a local dysfunction spreading from one tissue [42]. Through BM reconstitution in mice, we demonstrate a massive recruitment of CAFs from the BM. In contrast to previous published data [43,44], we show here that BM MSC engraftment is possible as assessed by the capacity of BM derived from chimeric mice to differentiate into mesenchymal cells. This observation is in line with the recent study of Quante et al. [40]. BM-derived CAFs expressed a fibroblastic marker (Thy1), a myofibroblastic marker (α-SMA), or a perivascular marker (NG2), indicating their contribution to the formation of both stromal septa and microvascular structures. In a model of chronic inflammation and gastric cancer progression, BM-derived cells were shown to differentiate to CAFs [40], as also evidenced in studies in other cancer models [45,46]. Recently, MSCs were also demonstrated to be pericytic precursors [47]. Our data reveal that around 30% of the α-SMA$^+$ myofibroblastic or NG2$^+$ pericytic cells that accumulate in the tumor-associated stroma are BM-derived, whereas only 10% of Thy1$^+$ fibroblast originate from the BM. Thy1 has been described as a marker of undifferentiated fibroblasts [48]. Indeed, higher α-SMA expression was found in Thy1-negative fibroblast subset, both at baseline and in response to transforming growth factor–β activation [48]. The stimulation of human pulmonary fibroblast with interleukin-1 and tumor necrosis factor–α promoted loss of Thy1 expression associated with differentiation to a myofibroblast phenotype [49]. Therefore, our results demonstrate that BM-derived cells contribute mainly to generate reactive fibroblasts and pericytes associated to vascular component.

We next focused our interest on MMP13, which has been demonstrated to be a key stromal mediator of cancer progression [29,50]. MMP13 is induced during invasion and metastasis of breast carcinoma, squamous cell carcinomas of the head and neck, and melanomas [21–26]. The human form of MMP13 has been evidenced in skin fibroblasts [51] and breast cancer cell–associated myofibroblasts [22,28]. Its expression has also been detected in cancer cells at the evading front. In accordance with previous reports [28,29], *in situ* hybridization combined with immunostaining revealed that MMP13 is produced by myofibroblasts. Notably, we found that MMP13 is produced by BM-derived myofibroblasts. This result, supported by combined *in situ* hybridization and immunostainings, suggests for the first time a specialization of a subpopulation of BM-derived CAFs in the production of MMP.

The concept of BM-derived MSCs as the source of MMP13 during cancer development is supported by *in vitro* experiments showing 1) MSC basal expression levels of MMP13 mRNA and proteins, which were strongly upregulated in co-culture with cancer cells; 2) the enhancement of squamous cell carcinoma spheroid migration in a collagen gel in the presence of wild-type but not MMP13-deficient MSC; 3) the inhibition of MSC-mediated tumor cell migration by a synthetic broad-spectrum MMP inhibitor. The pro-tumoral and pro-angiogenic role of stromal MMP13 in skin carcinoma development has previously been documented by subcutaneous injections of BDVII SCC tumor cells into wild-type or MMP13-deficient mice [29]. Similar results have also been reported for melanoma, where host MMP13 contributed to tumor vascularization and invasion [50]. Furthermore, in a model of choroidal neovascularization, we have previously demonstrated a pro-angiogenic role of MMP13, which was mediated by BM-derived mesenchymal cells [30]. In the present study, we provide evidence for the contribution of BM-derived cells to the constitution of the fibrovascular network and the involvement of these cells in cancer progression through MMP13 production. This work is in line with recent reports demonstrating the implication of BM-derived CAFs in tumor cell invasion [12,40].

In conclusion, our study strengthens the crucial contribution of BM-derived MSCs in cancer progression and invasion. The results strongly support a novel concept of BM-derived CAF specialization in tumor-supportive MMP production. Although MSCs have shown some clinical promise in cancer treatment [41] and is attracting the attention of researchers, the safety of such cell-based therapy that can generate cells producing pro-tumorigenic and pro-invasive MMPs must be assessed. Strategies that counteract MSC-cancer cell interactions appear of therapeutic value to block tumor cell invasiveness.

Acknowledgments

The authors acknowledge E. Feyereisen, M.-R. Pignon, E. Konradowski, M. Dehuy, G. Roland, P. Gavitelli, L. Poma, N. Lefin, and Ö. Turan for their collaboration and technical assistance. They thank Dr S. Ormenese and R. Stephan from the GIGA-Imaging and Flow Cytometry facility for their support with flow cytometry, as well as the GIGA-animal facility platform for their help.

References

[1] Joyce JA and Pollard JW (2009). Microenvironmental regulation of metastasis. *Nat Rev Cancer* **9**, 239–252.
[2] Hanahan D and Weinberg RA (2011). Hallmarks of cancer: the next generation. *Cell* **144**, 646–674.
[3] Carmeliet P and Jain RK (2011). Molecular mechanisms and clinical applications of angiogenesis. *Nature* **473**, 298–307.
[4] De Wever O, Demetter P, Mareel M, and Bracke M (2008). Stromal myofibroblasts are drivers of invasive cancer growth. *Int J Cancer* **123**, 2229–2238.
[5] Franco OE, Shaw AK, Strand DW, and Hayward SW (2010). Cancer associated fibroblasts in cancer pathogenesis. *Semin Cell Dev Biol* **21**, 33–39.
[6] Kalluri R and Zeisberg M (2006). Fibroblasts in cancer. *Nat Rev Cancer* **6**, 392–401.
[7] Tripathi M, Billet S, and Bhowmick NA (2012). Understanding the role of stromal fibroblasts in cancer progression. *Cell Adh Migr* **6**, 231–235.
[8] Kalluri R (2009). EMT: when epithelial cells decide to become mesenchymal-like cells. *J Clin Invest* **119**, 1417–1419.
[9] Wels J, Kaplan RN, Rafii S, and Lyden D (2008). Migratory neighbors and distant invaders: tumor-associated niche cells. *Genes Dev* **22**, 559–574.
[10] Zhu W, Xu W, Jiang R, Qian H, Chen M, Hu J, Cao W, Han C, and Chen Y (2006). Mesenchymal stem cells derived from bone marrow favor tumor cell growth *in vivo*. *Exp Mol Pathol* **80**, 267–274.
[11] Kidd S, Spaeth E, Dembinski JL, Dietrich M, Watson K, Klopp A, Battula VL, Weil M, Andreeff M, and Marini FC (2009). Direct evidence of mesenchymal stem cell tropism for tumor and wounding microenvironments using *in vivo* bioluminescent imaging. *Stem Cells* **27**, 2614–2623.
[12] De Boeck A, Pauwels P, Hensen K, Rummens JL, Westbroek W, Hendrix A, Maynard D, Denys H, Lambein K, Braems G, et al. (2012). Bone marrow-derived mesenchymal stem cells promote colorectal cancer progression through paracrine neuregulin 1/HER3 signalling. *Gut*, E-pub ahead of print.

[13] Mishra PJ, Mishra PJ, Humeniuk R, Medina DJ, Alexe G, Mesirov JP, Ganesan S, Glod JW, and Banerjee D (2008). Carcinoma-associated fibroblast–like differentiation of human mesenchymal stem cells. *Cancer Res* **68**, 4331–4339.

[14] Karnoub AE, Dash AB, Vo AP, Sullivan A, Brooks MW, Bell GW, Richardson AL, Polyak K, Tubo R, and Weinberg RA (2007). Mesenchymal stem cells within tumour stroma promote breast cancer metastasis. *Nature* **449**, 557–563.

[15] Beacham DA and Cukierman E (2005). Stromagenesis: the changing face of fibroblastic microenvironments during tumor progression. *Semin Cancer Biol* **15**, 329–341.

[16] Noel A, Jost M, and Maquoi E (2008). Matrix metalloproteinases at cancer tumor-host interface. *Semin Cell Dev Biol* **19**, 52–60.

[17] Aimes RT and Quigley JP (1995). Matrix metalloproteinase-2 is an interstitial collagenase. Inhibitor-free enzyme catalyzes the cleavage of collagen fibrils and soluble native type I collagen generating the specific 3/4- and 1/4-length fragments. *J Biol Chem* **270**, 5872–5876.

[18] Holmbeck K, Bianco P, Yamada S, and Birkedal-Hansen H (2004). MT1-MMP: a tethered collagenase. *J Cell Physiol* **200**, 11–19.

[19] Balbin M, Fueyo A, Tester AM, Pendas AM, Pitiot AS, Astudillo A, Overall CM, Shapiro SD, and Lopez-Otin C (2003). Loss of collagenase-2 confers increased skin tumor susceptibility to male mice. *Nat Genet* **35**, 252–257.

[20] Ala-aho R and Kahari VM (2005). Collagenases in cancer. *Biochimie* **87**, 273–286.

[21] Freije JM, Diez-Itza I, Balbin M, Sanchez LM, Blasco R, Tolivia J, and Lopez-Otin C (1994). Molecular cloning and expression of collagenase-3, a novel human matrix metalloproteinase produced by breast carcinomas. *J Biol Chem* **269**, 16766–16773.

[22] Airola K, Johansson N, Kariniemi AL, Kahari VM, and Saarialho-Kere UK (1997). Human collagenase-3 is expressed in malignant squamous epithelium of the skin. *J Invest Dermatol* **109**, 225–231.

[23] Nielsen BS, Rank F, Lopez JM, Balbin M, Vizoso F, Lund LR, Dano K, and Lopez-Otin C (2001). Collagenase-3 expression in breast myofibroblasts as a molecular marker of transition of ductal carcinoma *in situ* lesions to invasive ductal carcinomas. *Cancer Res* **61**, 7091–7100.

[24] Johansson N, Vaalamo M, Grenman S, Hietanen S, Klemi P, Saarialho-Kere U, and Kahari VM (1999). Collagenase-3 (MMP-13) is expressed by tumor cells in invasive vulvar squamous cell carcinomas. *Am J Pathol* **154**, 469–480.

[25] Airola K, Karonen T, Vaalamo M, Lehti K, Lohi J, Kariniemi AL, Keski-Oja J, and Saarialho-Kere UK (1999). Expression of collagenases-1 and -3 and their inhibitors TIMP-1 and -3 correlates with the level of invasion in malignant melanomas. *Br J Cancer* **80**, 733–743.

[26] Pendas AM, Uria JA, Jimenez MG, Balbin M, Freije JP, and Lopez-Otin C (2000). An overview of collagenase-3 expression in malignant tumors and analysis of its potential value as a target in antitumor therapies. *Clin Chim Acta* **291**, 137–155.

[27] Lafleur MA, Drew AF, de Sousa EL, Blick T, Bills M, Walker EC, Williams ED, Waltham M, and Thompson EW (2005). Upregulation of matrix metalloproteinases (MMPs) in breast cancer xenografts: a major induction of stromal MMP-13. *Int J Cancer* **114**, 544–554.

[28] Nielsen BS, Egeblad M, Rank F, Askautrud HA, Pennington CJ, Pedersen TX, Christensen IJ, Edwards DR, Werb Z, and Lund LR (2008). Matrix metalloproteinase 13 is induced in fibroblasts in polyomavirus middle T antigen-driven mammary carcinoma without influencing tumor progression. *PLoS One* **3**, e2959.

[29] Lederle W, Hartenstein B, Meides A, Kunzelmann H, Werb Z, Angel P, and Mueller MM (2010). MMP13 as a stromal mediator in controlling persistent angiogenesis in skin carcinoma. *Carcinogenesis* **31**, 1175–1184.

[30] Lecomte J, Louis K, Detry B, Blacher S, Lambert V, Bekaert S, Munaut C, Paupert J, Blaise P, Foidart JM, et al. (2011). Bone marrow-derived mesenchymal cells and MMP13 contribute to experimental choroidal neovascularization. *Cell Mol Life Sci* **68**, 677–686.

[31] Inada M, Wang Y, Byrne MH, Rahman MU, Miyaura C, Lopez-Otin C, and Krane SM (2004). Critical roles for collagenase-3 (Mmp13) in development of growth plate cartilage and in endochondral ossification. *Proc Natl Acad Sci USA* **101**, 17192–17197.

[32] Brouard N, Driessen R, Short B, and Simmons PJ (2010). G-CSF increases mesenchymal precursor cell numbers in the bone marrow via an indirect mechanism involving osteoclast-mediated bone resorption. *Stem Cell Res* **5**, 65–75.

[33] Fusenig NE, Amer SM, Boukamp P, and Worst PK (1978). Characteristics of chemically transformed mouse epidermal cells *in vitro* and *in vivo*. *Bull Cancer* **65**, 271–279.

[34] Lund LR, Romer J, Bugge TH, Nielsen BS, Frandsen TL, Degen JL, Stephens RW, and Dano K (1999). Functional overlap between two classes of matrix-degrading proteases in wound healing. *EMBO J* **18**, 4645–4656.

[35] Lund IK, Illemann M, Thurison T, Christensen IJ, and Hoyer-Hansen G (2011). uPAR as anti-cancer target: evaluation of biomarker potential, histological localization, and antibody-based therapy. *Curr Drug Targets* **12**, 1744–1760.

[36] Illemann M, Bird N, Majeed A, Laerum OD, Lund LR, Dano K, and Nielsen BS (2009). Two distinct expression patterns of urokinase, urokinase receptor and plasminogen activator inhibitor-1 in colon cancer liver metastases. *Int J Cancer* **124**, 1860–1870.

[37] Bisson C, Blacher S, Polette M, Blanc JF, Kebers F, Desreux J, Tetu B, Rosenbaum J, Foidart JM, Birembaut P, et al. (2003). Restricted expression of membrane type 1-matrix metalloproteinase by myofibroblasts adjacent to human breast cancer cells. *Int J Cancer* **105**, 7–13.

[38] Eccles SA, Box GM, Court WJ, Bone EA, Thomas W, and Brown PD (1996). Control of lymphatic and hematogenous metastasis of a rat mammary carcinoma by the matrix metalloproteinase inhibitor batimastat (BB-94). *Cancer Res* **56**, 2815–2822.

[39] Wang SS, Asfaha S, Okumura T, Betz KS, Muthupalani S, Rogers AB, Tu S, Takaishi S, Jin G, Yang X, et al. (2009). Fibroblastic colony-forming unit bone marrow cells delay progression to gastric dysplasia in a helicobacter model of gastric tumorigenesis. *Stem Cells* **27**, 2301–2311.

[40] Quante M, Tu SP, Tomita H, Gonda T, Wang SS, Takashi S, Baik GH, Shibata W, Diprete B, Betz KS, et al. (2011). Bone marrow-derived myofibroblasts contribute to the mesenchymal stem cell niche and promote tumor growth. *Cancer Cell* **19**, 257–272.

[41] Studeny M, Marini FC, Dembinski JL, Zompetta C, Cabreira-Hansen M, Bekele BN, Champlin RE, and Andreeff M (2004). Mesenchymal stem cells: potential precursors for tumor stroma and targeted-delivery vehicles for anticancer agents. *J Natl Cancer Inst* **96**, 1593–1603.

[42] McAllister SS and Weinberg RA (2010). Tumor-host interactions: a far-reaching relationship. *J Clin Oncol* **28**, 4022–4028.

[43] Simmons PJ, Przepiorka D, Thomas ED, and Torok-Storb B (1987). Host origin of marrow stromal cells following allogeneic bone marrow transplantation. *Nature* **328**, 429–432.

[44] Yokota T, Kawakami Y, Nagai Y, Ma JX, Tsai JY, Kincade PW, and Sato S (2006). Bone marrow lacks a transplantable progenitor for smooth muscle type alpha-actin-expressing cells. *Stem Cells* **24**, 13–22.

[45] Direkze NC, Hodivala-Dilke K, Jeffery R, Hunt T, Poulsom R, Oukrif D, Alison MR, and Wright NA (2004). Bone marrow contribution to tumor-associated myofibroblasts and fibroblasts. *Cancer Res* **64**, 8492–8495.

[46] Guo X, Oshima H, Kitmura T, Taketo MM, and Oshima M (2008). Stromal fibroblasts activated by tumor cells promote angiogenesis in mouse gastric cancer. *J Biol Chem* **283**, 19864–19871.

[47] Jeon ES, Moon HJ, Lee MJ, Song HY, Kim YM, Cho M, Suh DS, Yoon MS, Chang CL, Jung JS, et al. (2008). Cancer-derived lysophosphatidic acid stimulates differentiation of human mesenchymal stem cells to myofibroblast-like cells. *Stem Cells* **26**, 789–797.

[48] Zhou Y, Hagood JS, and Murphy-Ullrich JE (2004). Thy-1 expression regulates the ability of rat lung fibroblasts to activate transforming growth factor-beta in response to fibrogenic stimuli. *Am J Pathol* **165**, 659–669.

[49] Hagood JS, Prabhakaran P, Kumbla P, Salazar L, MacEwen MW, Barker TH, Ortiz LA, Schoeb T, Siegal GP, Alexander CB, et al. (2005). Loss of fibroblast Thy-1 expression correlates with lung fibrogenesis. *Am J Pathol* **167**, 365–379.

[50] Zigrino P, Kuhn I, Bauerle T, Zamek J, Fox JW, Neumann S, Licht A, Schorpp-Kistner M, Angel P, and Mauch C (2009). Stromal expression of MMP-13 is required for melanoma invasion and metastasis. *J Invest Dermatol* **129**, 2686–2693.

[51] Toriseva MJ, Ala-aho R, Karvinen J, Baker AH, Marjomaki VS, Heino J, and Kahari VM (2007). Collagenase-3 (MMP-13) enhances remodeling of three-dimensional collagen and promotes survival of human skin fibroblasts. *J Invest Dermatol* **127**, 49–59.